Theory of the reactant-stationary kinetics for a coupled auxiliary enzyme assay

Justin Eilertsen[a], Wylie Stroberg[a], Santiago Schnell[a,b,c,1]

[a]*Department of Molecular & Integrative Physiology, University of Michigan Medical School, Ann Arbor, MI 48109, USA*
[b]*Department of Computational Medicine & Bioinformatics, University of Michigan Medical School, Ann Arbor, MI 48109, USA*
[c]*Brehm Center for Diabetes Research, University of Michigan Medical School, Ann Arbor, MI 48105, USA*

Abstract

A theoretical analysis is performed on the nonlinear ordinary differential equations that govern the dynamics of a coupled auxiliary enzyme catalyzed reaction. The assay consists of a non-observable reaction and an indicator (observable) reaction, where the product of the first reaction is the enzyme for the second. Both reactions are governed by the single substrate, single enzyme Michaelis–Menten reaction mechanism. Using singular perturbation methods, we derive asymptotic solutions that are valid under the quasi-steady-state and reactant-stationary assumptions. In particular, we obtain closed form solutions, analogous to the Schnell–Mendoza equation for Michaelis–Menten type reactions, that approximate the evolution of the observable reaction. Conditions for the validity of the asymptotic solutions are also rigorously derived showing that these asymptotic expressions are applicable under the reactant-stationary kinetics.

Keywords: Coupled enzyme assay, time course experiments, timescale separation analysis, singular perturbation analysis, Schnell–Mendoza equation

Email address: schnells@umich.edu (Santiago Schnell)
[1]Corresponding author

1. Introduction

Difficult detectable or non-observable enzyme reactions are frequently coupled with easily observable reactions to be studied in enzyme kinetic experiments; the hope is that the enzyme activity of the non-observable reaction can be measured by analyzing the progress curves of the secondary observable reaction. Traditionally, coupled assays are designed in the *sequential* form (see [1] for specific applications), in which the product of the non-observable reaction is a substrate that is catalyzed by a second, sequential enzyme. In addition to the well-studied sequential assay [2, 3, 4, 5], there is also the *auxiliary* enzyme assay. In this assay, the primary enzyme, E_1, reacts with the substrate S_1 to form an intermediate complex C_1 following the Michaelis–Menten (MM) [6] mechanism. The product of the primary reaction is thus the activated form of the secondary enzyme, E_2:

$$E_1 + S_1 \underset{k_{-1}}{\overset{k_1}{\rightleftharpoons}} C_1 \overset{k_2}{\rightarrow} E_1 + E_2 \ . \tag{1}$$

The first (primary) reaction (1) represents a non-observable enzyme catalyzed reaction. In the secondary reaction, the substrate S_2 binds with the enzyme E_2 to form a complex C_2, which will synthesize the product, P, and release the enzyme, E_2 in the catalytic step of the reaction:

$$E_2 + S_2 \underset{k_{-3}}{\overset{k_3}{\rightleftharpoons}} C_2 \overset{k_4}{\rightarrow} E_2 + P \ . \tag{2}$$

Mechanism (2) represents the observable reaction, which is is generally known as the *indicator* reaction. In this coupled enzyme assay, the product enzyme, E_2, of the non-observable reaction is known as an auxiliary enzyme, because it provides support to measure the non-observable reaction through the indicator reaction. In the above chemical steps, k_1, k_{-1}, k_3, k_{-3} are microscopic rate constants, and k_2, k_4 are catalytic constants.

The auxiliary reaction mechanism (1)–(2) occurs naturally in coagulation cascades [7]. As a distinct example, the activation of protein C (PC) by thrombin (T) follows a reaction consistent with (1):

$$T + PC \underset{k_{-1}}{\overset{k_1}{\rightleftharpoons}} TPC \overset{k_2}{\rightarrow} T + APC \tag{3}$$

where "APC" denotes the activated form of PC. In the experimental assay, the activated enzyme APC then catalyzes a substrate (S). Assuming S is specific to APC and thus does not bind with T, the secondary, observable reaction follows the form of (2),

$$APC + S \underset{k_{-3}}{\overset{k_3}{\rightleftharpoons}} SAPC \overset{k_4}{\rightarrow} APC + P\ . \tag{4}$$

Experimentally, the kinetics of the non-observable reaction is measured by decoupling the analysis of progress curves by adding excessive concentrations of the primary enzyme, and making the first reaction pseudo-first order [7]. There has been a reasonable amount of literature that features kinetic modeling of coagulation cascades [8, 9, 10], but complex cascade kinetic models have limited applicability to the parameter estimation of enzyme assays, like the auxiliary reaction mechanism (1)–(2). Derivation of rate equations for coupled enzyme assays has been primarily limited to the sequential enzyme system [4, 5, 2], rather than the auxiliary enzyme assay due to the complex non-linear coupling of the differential equations governing the kinetic of the reaction mechanism.

Under appropriate conditions, the rate of substrate depletion for the non-observable reaction is described by the MM equation,

$$\dot{s}_1 = -\frac{V_1}{K_{M_1} + s_1} s_1 \tag{5}$$

where s_1 is the concentration of S_1, $K_{M_1} = (k_{-1} + k_2)/k_1$ is the Michaelis constant, and $V_1 = k_2 e_1^0$ is limiting rate of the reaction, which is dependent on

both the catalytic constant k_2 and the initial concentration of E_1 (the initial concentration of E_1 is denoted as e_1^0). Of great interest to both theoreticians [11, 12] and experimentalists is the estimation of the constants K_{M_1} and V_1 from the so-called *inverse problem*. The inverse problem is carried out in two stages: First, experimental data is produced in the form of a progress curve for either s_1 or p (we have used lower case letters to denote the concentrations of S_1 and P respectively). Second, the experimental data is then used to try and estimate both K_{M_1} and V_1 by optimally *fitting* the model (5) through the utilization of either a deterministic (i.e., such as Levenburg-Marquardt) or a stochastic (Markov Chain Monte Carlo) algorithm. In general, one seeks to estimate kinetic constants with an expression contains the fewest number of parameters; this is why the MM equation is more attractive than the complete set of mass action equations. The MM equation is what is known as a *reduced model*, and it is *reduced* in the sense that it contains fewer variables (s_1 versus s_1 *and* c_1) and fewer parameters (K_{M_1} and V_1 versus k_1, k_{-1} and k_2).

The inverse problem presents a unique challenge for both experimentalists and theorists. First, the parameters that govern the enzyme activity of the non-observable reaction must somehow be determined from the indicator reaction, since in a typical in vitro laboratory experiment, progress curves can only be generated for the indicator reaction. Second, a reduced model for coupled auxiliary enzyme reactions must be developed. The reduced model should, (1) decrease the number of variables, and (2) lessen the number of parameters needed to describe the time course of the complete auxiliary reaction.

1.1. Enzyme kinetic rate equations are reduced models resulting from scaling and simplification analysis

The MM equation is the result of a model reduction method known as *slow manifold projection*. The validity of the MM equation resides under the assumption that the single-enzyme, single-substrate reaction (1 has two intrinsic timescales. The first timescale is very short, and accounts for the rapid accumulation of the complex C_1. The second timescale is very long, and gives a rough

measure of the time it takes for the completion of the reaction. Respectively, these timescales are known as *fast* and *slow* timescales. If these timescales are inherently present within (1), then the dimensionless mass action equations that model (1 can be written in the form

$$\begin{aligned} \dot{s}_1 &= f_1(s_1, c_1) \\ \varepsilon \dot{c}_1 &= f_2(s_1, c_1) \end{aligned} \tag{6}$$

where ε is very small (i.e., $\varepsilon \ll 1$), and is proportional to the ratio of the fast timescale to the slow timescale. Differential equations in the form of (6) are called singularly perturbed differential equations, and they are ubiquitous in mathematical chemistry [13, 14, 15] and biology [16]. Thus, central to deriving a reduced model for the auxiliary reaction (using slow manifold projection) is the estimation of the slow and fast timescales for the non-observable reaction. This is challenging for coupled reactions, since the time to completion of the indicator reaction can occur before, after, or at approximately the same time as the non-observable reaction. Furthermore, it is unlikely that the relative speeds and completion time of the non-observable reaction (1) will be known. Thus, there is a need derive a reduced model that is general enough so that its validity is certain regardless of which reaction is fastest. Finally, the most desirable reduced model will be one in which a closed form solution is obtainable so that the reduced model may be expressed as an explicit function of time. This will eliminate the need to generate *explicit* progress curves for s_1, since the time course of s_1 is non-observable and consequently unknown.

1.2. Goals of this work

Up to date, the reduction theoretical analysis of auxiliary enzyme catalyzed reactions has been limited to first-order kinetics models [4, 5, 3], which has a limited validity in time course experiments [17]. Through singular perturbation methods, we will show that the complete (coupled) system that includes both the non-observable and indicator reaction can be reduced to a system of the

form

$$\begin{aligned} \dot{s}_1 &= f(s_1; K_{M_1}, V_1) \\ \dot{s}_2 &= g(s_1, s_2; K_{M_1}, K_{M_2}, V_1, V_2) \end{aligned} \tag{7}$$

where $K_{M_2} = (k_{-3} + k_4)/k_3$ is the Michaelis constant of the indicator reaction, and $V_2 = k_4 s_1^0$ is the limiting rate of the indicator reaction (s_1^0 denotes the initial concentration of S_1). The reduced model (7) admits closed-form solutions in the form of a Schnell–Mendoza equation [18]; conditions for the validity of the reduced model will be established, and timescale estimates will be derived. In addition, we will exploit the geometry of the mathematical structure [19, 20] in extreme situations when the speeds of the reactions are significantly disparate; this will allow us to "simplify" the reduced model and obtain asymptotic solutions that are in some ways easier in form than both the general reduced model and the system of mass action equations. Finally, in Section 6, we conclude with a brief discussion of the results and their relevance in possible future work involving the inverse problem.

2. Derivation of the governing equations for the coupled auxiliary enzyme reactions

Applying the law of mass action to coupled auxiliary enzyme reaction mechanism (1)–(2) yields seven rate equations

$$\dot{e_1} = -k_1 e_1 s_1 + (k_{-1} + k_2) c_1 \tag{8a}$$

$$\dot{s_1} = -k_1 e_1 s_1 + k_{-1} c_1 \tag{8b}$$

$$\dot{c_1} = k_1 e_1 s_1 - (k_{-1} + k_2) c_1 \tag{8c}$$

$$\dot{e_2} = k_2 c_1 - k_3 e_2 s_2 + (k_{-3} + k_4) c_2 \tag{8d}$$

$$\dot{s_2} = -k_3 e_2 s_2 + k_{-3} c_2 \tag{8e}$$

$$\dot{c_2} = k_3 e_2 s_2 - (k_{-3} + k_4) c_2 \tag{8f}$$

$$\dot{p} = k_4 c_2, \tag{8g}$$

where lowercase letters represent concentrations of the corresponding uppercase species. Typically, laboratory enzyme assays present the following initial

conditions

$$(e_1, s_1, c_1, e_2, s_2, c_2, p)\,|_{t=0} = \left(e_1^0, s_1^0, 0, 0, s_2^0, 0, 0\right). \tag{9}$$

By examining the system of rate equations (8), the coupled auxiliary enzyme reaction mechanism obeys three conservation laws:

$$e_1\,(t) + c_1\,(t) = e_1^0, \tag{10a}$$

$$s_1\,(t) + c_1\,(t) + c_2\,(t) + e_2\,(t) = s_1^0, \tag{10b}$$

$$s_2\,(t) + c_2\,(t) + p\,(t) = s_2^0. \tag{10c}$$

Mathematically speaking, the solution trajectory to (8) must lie on the intersection of the hyperplanes defined in (10), which means the original seven-dimensional problem can be reduced to a four-dimensional problem. Using (10a) and (10b) to decouple the enzyme concentrations, the redundancies in the system (8) are eliminated to yield

$$\dot{s_1} = -k_1\left(e_1^0 - c_1\right)s_1 + k_{-1}c_1 \tag{11a}$$

$$\dot{c_1} = k_1\left(e_1^0 - c_1\right)s_1 - \left(k_{-1} + k_2\right)c_1 \tag{11b}$$

$$\dot{s_2} = -k_3(s_1^0 - s_1 - c_1 - c_2)s_2 + k_{-3}c_2 \tag{11c}$$

$$\dot{c_2} = k_3(s_1^0 - s_1 - c_1 - c_2)s_2 - (k_{-3} + k_4)c_2, \tag{11d}$$

where $e_1(t)$, $e_2(t)$ and $p(t)$ are readily calculated once $s_1(t)$, $c_1(t)$, $s_2(t)$ and $c_2(t)$ are known.

3. Rate expressions for the non-observable enzyme catalyzed reaction

The rate equations (11a)–(11b) are uncoupled from (11c)–(11d). These rate equations have the same structure to those of the single-substrate, single-enzyme reaction following the MM mechanism. Therefore, it is possible to derive rate equations to model the coupled auxiliary enzyme catalyzed reaction, and estimate its kinetic parameters using the general theory of the reactant-stationary assumption (RSA, [21]). The rate equations for the non-observable reaction are identical to those of the single substrate, single enzyme reaction following the MM mechanisms.

3.1. Review of the single substrate, single enzyme MM reaction

Revisiting the analysis for the single-substrate, single-enzyme reaction, it has long been established that there there can be a rapid buildup of c_1 during an initial fast transient of the non-observable reaction. After this rapid buildup (where the rate of depletion of c_1 approximately equals its rate of formation) c_1 is assumed to be in a quasi-steady-state (QSS),

$$\dot{c_1} \approx 0 \quad \text{for} \quad t > t_{c_1}. \tag{12}$$

The timescale t_{c_1} is the time associated with the initial transient buildup of c_1,

$$t_{c_1} = \frac{1}{k_1(K_{M_1} + s_1^0)}. \tag{13}$$

The quasi-steady-state assumption (QSSA, 12), in combination with (11a)–(11b), leads to the derivation of the well-known rate expressions,

$$c_1 = \frac{e_1^0 s_1}{K_{M_1} + s_1} \tag{14a}$$

$$\dot{s_1} = -\frac{V_1 s_1}{K_{M_1} + s_1}, \tag{14b}$$

from which we see that the mass action equations (11a)–(11b) are reduced to a differential-algebraic equation systems with one single differential equation for s_1.

Since equations (14a) and (14b) are only valid after the initial transient, t_{c_1}, it is necessary to define a boundary condition for s_1 at $t = t_{c_1}$. This is equivalent to the initial experimental condition for the initial rate or time course experiments. To find this condition, it can be assumed that there is a negligible decrease in s_1 during the initial transient. This is known as the RSA, and is expressed as

$$s_1(t < t_{c_1}) \approx s_1^0. \tag{15}$$

The RSA provides an initial condition for (11a) under the variable transformation $\hat{t} \mapsto t - t_{c_1}$. The mathematical expression (14b) is the MM equation, and the system (14a)–(14b) governs the dynamics of the substrate s_1 and complex c_1

of the observable reaction under the QSS and RSA. The *explicit* closed-form solution of (14b), with the initial condition (15), is known as the Schnell–Mendoza equation [18], and is written in terms of the Lambert-W function

$$\frac{s_1\left(\hat{t}\right)}{K_{M_1}} = W\left[\sigma_1 \exp(\sigma_1 - \eta_1 \hat{t})\right], \quad \sigma_1 = \frac{s_1^0}{K_{M_1}}, \quad \eta_1 = \frac{V_1}{K_{M_1}}. \tag{16}$$

From the perspective of asymptotic theory, Schnell and Mendoza [18] have provided a piecewise solution for the MM reaction in terms of a fast transient solution for s_1, valid for $t \leq t_{c_1}$, as well as a QSS solution for s_1, valid for $t > t_{c_1}$:

$$s_1 = s_1^0, \quad t \leq t_{c_1} \tag{17a}$$

$$s_1 = K_{M_1} W\left[\sigma_1 \exp(\sigma_1 - \eta_1 \hat{t})\right], \quad t > t_{c_1} \tag{17b}$$

From the earlier work of Segel [22], we have a *fast* solution, valid when $t \leq t_{c_1}$, for the complex c_1, as well as a QSS solution which is valid for $t > t_{c_1}$,

$$c_1 = \bar{c}_1\left[1 - \exp(-t/t_{c_1})\right], \quad t < t_{c_1}, \quad \bar{c}_1 = \frac{e_1^0}{K_{M_1} + s_1^0} s_1^0 \tag{18a}$$

$$c_1 = \frac{e_1^0 s_1}{K_{M_1} + s_1}, \quad t \geq t_{c_1}. \tag{18b}$$

Collectively, equations (17a) and (18b) constitute an *asymptotic* solution that serves as an accurate approximation to the full time course of (11), provided the appropriate qualifiers (i.e, the RSA and the QSSA) are obeyed.

In addition to the timescale t_{c_1}, which quantifies the length of the initial fast transient (build-up of c_1), the time it takes for the majority of the substrate s_1 to be depleted is given by t_{s_1}. Although there are several methods for estimating the significant timescales of chemical reactions [23], we employ the heuristic method proposed by Segel [22], and approximate the depletion time to be effectively the total depletion of s_1 (the total depletion is s_1^0) divided by the maximum rate of substrate of depletion after t_{c_1}:

$$t_{s_1} = \frac{\Delta s_1}{\max\limits_{0 \leq t} |\dot{s}_1|} = \frac{K_{M_1} + s_1^0}{V_1}. \tag{19}$$

Generally speaking, t_{s_1} is a reasonable measure of how long it takes for the non-observable reaction to complete.

3.2. Geometrical picture of the enzyme catalyzed reaction, and conditions for the validity of asymptotic solutions of the rate equations

While the asymptotic solutions are useful in that they can be employed to make certain predictions about the behavior of the reaction, asymptotic theory fails to yield a visual or geometric understanding of the dynamical behavior of the coupled enzyme auxiliary reaction mechanism. To paint a complete picture of the mathematical structure behind the reaction mechanism (1)–(2), we turn to dynamical systems theory, and analyze this problem from phase-space. From this perspective, after the initial buildup of c_1, the phase-space trajectory of the non-observable reaction (11a)–(11b) *hugs* a slow manifold, '$\mathcal{M}_\varepsilon$,' and is asymptotic to $\mathcal{M}_\varepsilon$ in the approach to equilibrium. The time it takes for the trajectory to reach the slow manifold is approximately t_{c_1}, while the time it takes for the trajectory to equilibrium is approximated by t_{s_1}. The condition for the validity of the asymptotic solution resides in *how well* the c_1-nullcline approximates the slow manifold, $\mathcal{M}_\varepsilon$, and also *how straight* the phase-space trajectory is in its approach to the slow manifold during the initial *fast* transient. The former of these conditions is known as the *QSSA*, and the latter is of course the geometrical interpretation of the *RSA*. We note that, chemically speaking, if the trajectory is close the slow manifold $\mathcal{M}_\varepsilon$, then the complex C_1 is assumed to be in a QSS for which the difference and the rate of C_2 depletion is approximately equal to the rate C_2 formation. Mathematically, it was originally proposed that the QSSA was valid if $t_{c_1} \ll t_{s_1}$,

$$\frac{1}{k_1(K_{M_1} + s_1^0)} \ll \frac{K_{M_1} + s_1^0}{V_1}. \tag{20}$$

In other words, it was assumed that the c_1-nullcline should be considered a *good* approximation to the slow manifold $\mathcal{M}_\varepsilon$ if the timescale accounting for the build-up of c_1 was small compared to the timescale accounting for the duration of the reaction.

As for the validity of the RSA, Segel [24] proposed that one could assume little change in s_1 (an almost *straight* phase-space trajectory towards the slow manifold) if the depletion of s_1 over the timescale t_{c_1} is minimal:

$$\max_{t\geq 0}|\dot{s}_1|\cdot t_{c_1} \ll s_1^0. \tag{21}$$

Since $|\dot{s}_1| \leq s_1^0 e_1^0$, the strict inequality given in (21) translates to,

$$\frac{e_1^0}{K_{M_1}+s_1^0} \equiv \varepsilon \ll 1. \tag{22}$$

Through scaling analysis, Segel [22] went on to show that the RSA, $\varepsilon \ll 1$, determines single-handedly the validity of the asymptotic solutions (17) and (18). Introducing the dimensionless variables $\hat{s}_1 = s_1/s_1^0$ and $\hat{c}_1 = c_1/\bar{c}_1$, Segel and Slemrod [24] demonstrated that, with respect to the dimensionless timescale $\tau = t/t_{c_1}$, equations (11a)-(11a) scale as

$$\frac{d\hat{s}_1}{d\tau} = \varepsilon\left[-\hat{s}_1 + \frac{\sigma_1}{\sigma_1+1}\hat{c}_1\hat{s}_1 + \frac{\kappa_1(1+\kappa_1)^{-1}}{\sigma_1+1}\hat{c}_1\right] \tag{23a}$$

$$\frac{d\hat{c}_1}{d\tau} = \hat{s}_1 - \frac{\sigma_1}{\sigma_1+1}\hat{c}_1\hat{s}_1 - \frac{1}{\sigma_1+1}\hat{c}_1, \tag{23b}$$

where $\kappa_1 = k_{-1}/k_2$ and $\varepsilon = e_1^0/(k_{M_1}+s_1^0)$. In contrast, under the timescale $T = t/t_{s_1}$, (11a)-(11a) become:

$$\frac{d\hat{s}_1}{dT} = (\kappa_1+1)(\sigma_1+1)\left[-\hat{s}_1 + \frac{\sigma_1}{\sigma_1+1}\hat{c}_1\hat{s}_1 + \frac{\kappa_1(1+\kappa_1)^{-1}}{\sigma_1+1}\hat{c}_1\right] \tag{24a}$$

$$\varepsilon\frac{d\hat{c}_1}{dT} = (\kappa_1+1)(\sigma_1+1)\left[\hat{s}_1 - \frac{\sigma_1}{\sigma_1+1}\hat{c}_1\hat{s}_1 - \frac{1}{\sigma_1+1}\hat{c}_1\right]. \tag{24b}$$

Thus, it is apparent from the dimensionless equations (23)-(24b), that if $\varepsilon \ll 1$, then not only will the RSA hold, but the QSSA (which assumes that the c_1-nullcline is a good approximation to $\mathcal{M}_\varepsilon$) also holds. In fact, the RSA, $\varepsilon \ll 1$, is more restrictive than separation of timescales. After some algebraic calculations, the separation of timescales, $t_{c_1}/t_{s_1} \ll 1$, can be written as:

$$\frac{e_1^0}{K_{M_1}+s_1^0} \ll \left(1+\frac{K_{S_1}}{K_1}\right)\left(1+\frac{s_1^0}{K_{M_1}}\right), \tag{25}$$

where $K_{S_1} = k_{-1}/k_1$, and $K_1 = k_2/k_1$. For the RSA to be valid, the condition

$$\frac{e_1^0}{K_{M_1}} \ll \left(1 + \frac{s_1^0}{K_{M_1}}\right), \tag{26}$$

must be satisfied, which is more stringent than condition (25), and hence dictates the conditions under which equation (14b) or (16) can be applied. For this reason, it is nowadays considered that MM expressions are valid under the RSA (see FIGURES 1a and 1b), rather than the QSSA [25].

3.3. Scaling analysis of the indicator reaction

The scaling analysis of the indicator reaction requires knowledge of fast and slow timescales, as well as knowledge of reasonable upper and lower bounds of s_2 and c_2. We will start by trying to estimate a slow timescale for the indicator reaction. An accurate slow timescale should give us a reasonable estimation of the completion time for the indicator reaction (in the case of the auxiliary reaction, the completion of the indicator reaction can be faster, as fast, or slower than the non-observable reaction). For the non-observable reaction, the slow timescale is expressed in terms of the initial quantities s_1^0 and e_1^0, and the Michaelis constant K_{M_1}:

$$t_{s_1} = \frac{K_{M_1} + s_1^0}{V_1}. \tag{27}$$

The quantity e_1^0 is the total amount of enzyme for the non-observable reaction. The construction of a homologous slow timescale for the indicator reaction is problematic in that the total amount of available enzyme e_2^A,

$$e_2^A(t) = s_1^0 - s_1 - c_1, \tag{28}$$

is a time-dependent quantity. We will employ a mean-field approach to derive a slow (depletion) timescale for the indicator reaction. Let us first assume that we know the slow timescale for indicator reaction, and denote this timescale as T_{s_2}. Then, the mean available enzyme over the time course of the indicator reaction, which we will denote as $\langle e_2^A \rangle$, is given by

$$\langle e_2^A \rangle = \frac{1}{T_{s_2}} \int_0^{T_{s_2}} e_2^A(t)\, \mathrm{d}t. \tag{29}$$

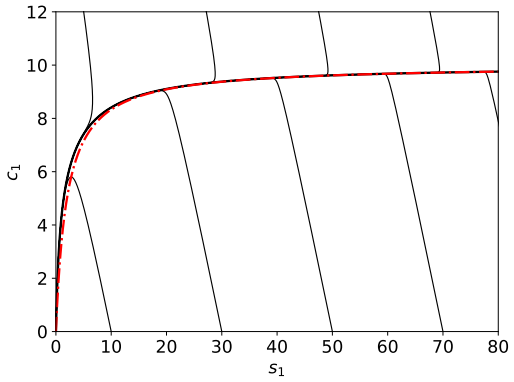

(a)

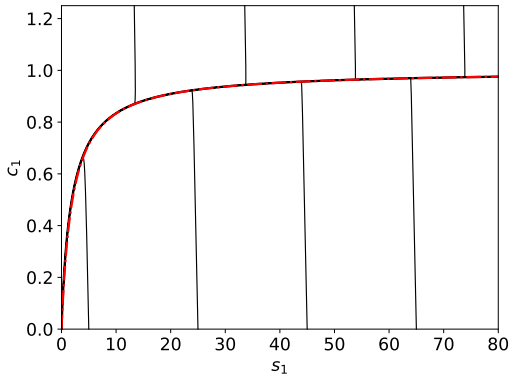

(b)

Figure 1: Geometrical picture of the single-substrate, single-enzyme non observable reaction (1). (a) Phase space dynamics with $e_1^0 = 10, k_1 = 1, k_2 = 1$ and $k_{-1} = 1$. (b) Phase space dynamics with $e_1^0 = 1, s_1^0 = 78, k_1 = 1, k_2 = 5$ and $k_{-1} = 1$. As $\varepsilon \to 0$, the accumulation of c_1 is more rapid, and the c_1-nullcline (dashed red curve) becomes a better approximation to the slow manifold, $\mathcal{M}_\varepsilon$, which is the thick black curve. The slow manifold curve is a graphical representation of the steady-state kinetic rate equation. The thin black curves are trajectories starting from different initial conditions, and represent the fast-transient kinetics of the reaction.

If the completion of the indicator reaction occurs long before the completion of the non-observable reaction, then we should expect that $\langle e_2^A \rangle \ll s_1^0$. In contrast, if the completion of the indicator reaction occurs long after the completion of the non-observable reaction, then would should expect $\langle e_2^A \rangle \approx s_1^0$. In any case,

we can define the slow timescale as

$$T_{s_2} = \frac{K_{M_2} + s_2^0}{k_4 \langle e_2^A \rangle}, \tag{30}$$

which should yield a reasonable estimate for the slow timescale *if* the depletion of s_2 is influenced by a slow manifold.

Next, we want to scale the mass action equations that model the indicator reaction with respect to the quantities $\mathbb{T} = t/\hat{t}$, s_2^0, and $\max e_2^A$, where $\max e_2^A$ is the maximum amount of e_2^A over the course of the indicator reaction:

$$\max e_2^A \equiv \max_{t \leq T_{s_2}} (s_1^0 - s_1 - c_1). \tag{31}$$

Utilizing $\max e_2^A$ as an upper bound on the available enzyme dictates a natural scaling of c_2,

$$c_2 \leq \frac{\max e_2^A}{K_{M_2} + s_2^0} s_2^0 \equiv \hat{c}_2. \tag{32}$$

Next, we scale the mass action equations with respect to the following dimensionless variables,

$$\bar{s}_2 s_2^0 = s_2, \quad \bar{c}_2 \hat{c}_2 = c_2, \quad \bar{e}_2^A \max e_2^A = e_2^A, \quad \mathbb{T}\hat{t} = t, \tag{33}$$

where $\hat{t}$ denotes an arbitrary timescale. Substitution of these quantities into the mass action equation yields

$$\frac{d\bar{s}_2}{d\mathbb{T}} = \frac{\max e_2^A}{\langle e_2^A \rangle} \frac{\hat{t}}{T_{s_2}} (1+\kappa_2)(1+\sigma_2) \left[\left(\frac{\sigma_2}{1+\sigma_2} \bar{c}_2 - \bar{e}_2^A \right) \bar{s}_2 + \frac{\alpha}{1+\sigma_2} \bar{c}_2 \right] \tag{34a}$$

$$\lambda \frac{d\bar{c}_2}{d\mathbb{T}} = \frac{\max e_2^A}{\langle e_2^A \rangle} \frac{\hat{t}}{T_{s_2}} (1+\kappa_2)(1+\sigma_2) \left[\left(\bar{e}_2^A - \frac{\sigma_2}{1+\sigma_2} \bar{c}_2 \right) \bar{s}_2 - \frac{1}{1+\sigma_2} \bar{c}_2 \right]. \tag{34b}$$

In the above expressions, the dimensionless quantities σ_2, κ_2 and α are:

$$\sigma_2 = s_2^0 / K_{M_2}, \quad \kappa_2 = k_{-3}/k_4, \quad \alpha = \kappa_2/(1+\kappa_2). \tag{35}$$

The parameter λ, defined as

$$\lambda = \frac{\max e_2^A}{K_{M_2} + s_2^0}, \tag{36}$$

is unique in that if it is sufficiently small, then it mathematically characterizes the indicator reaction as a singularly perturbed differential equation for which model reduction is possible through means of projecting onto the slow manifold, "$\mathcal{M}_\lambda$."

4. Asymptotic analysis of the coupled auxiliary enzyme system

Now that we have a good idea as to how the mass action equations of the indicator reaction scale, we want to try and find closed-form asymptotic solutions to the mass action equations or, at the very least, try and reduce the dimension of the mass action differential equations. The exact form of the scaled mass action equations will depend on the slow timescales of both the observable and non-observable indicator reactions. Thus, given that the respective slow timescale of the indicator and non-observable reactions are T_{s_2} and t_{s_1}, we will analyze

$$\frac{d\bar{s}_2}{dT} = \frac{\max e_2^A}{\langle e_2^A \rangle}\frac{(1+\kappa_2)(1+\sigma_2)}{\delta_S}\left[\left(\frac{\sigma_2}{\sigma_2+1}\bar{c}_2 - \bar{e}_2^A\right)\bar{s}_2 + \frac{\alpha}{\sigma_2+1}\bar{c}_2\right] \tag{37a}$$

$$\lambda\frac{d\bar{c}_2}{dT} = \frac{\max e_2^A}{\langle e_2^A \rangle}\frac{(1+\kappa_2)(1+\sigma_2)}{\delta_S}\left[\left(\bar{e}_2^A - \frac{\sigma_2}{\sigma_2+1}\bar{c}_2\right)\bar{s}_2 - \frac{1}{\sigma_2+1}\bar{c}_2\right], \tag{37b}$$

where δ_S is the ratio of the substrate depletion timescales, $\delta_S = T_{s_2}/t_{s_1}$, and $T = t/t_{s_1}$. Based on the scaling given in (37a) and (37b, we will derive an estimate for T_{s_2} as well as solutions for three particular cases, which are defined by the scale of δ_S: (i) **Case 1:** the indicator reaction is faster than the non-observable reaction ($\delta_S \ll 1$), **Case 2:** the indicator reaction is roughly the same speed as the non-observable reaction ($\delta_S \approx 1$), and **Case 3:** the indicator reaction is much slower than the non-observable reaction ($\delta_S \gg 1$).

4.1. Case 1: The indicator reaction is faster than the non-observable reaction ($\delta_S \ll 1$)

If the indicator reaction is fast, and $\delta_S \ll 1$, then the dominant slow timescale is t_{s_1}, and thus the completion of the non-observable reaction will

occur long after the completion of the indicator reaction. To start the analysis, we will rescale the mass action equations that govern the non-observable reaction with respect to $\hat{T} = t/T_{s_2}$:

$$\frac{d\hat{s}_1}{d\hat{T}} = \delta_S(1+\kappa_1)(1+\sigma_1)\left[-\hat{s}_1 + \frac{\sigma_1}{\sigma_1+1}\hat{c}_1\hat{s}_1 + \frac{\kappa_1(1+\kappa_1)^{-1}}{\sigma_1+1}\hat{c}_1\right] \tag{38a}$$

$$\varepsilon\frac{d\hat{c}_1}{d\hat{T}} = \delta_S(1+\kappa_1)(1+\sigma_1)\left[\hat{s}_1 - \frac{\sigma_1}{\sigma_1+1}\hat{c}_1\hat{s}_1 - \frac{1}{\sigma_1+1}\hat{c}_1\right]. \tag{38b}$$

By inspection of (38a, if $\delta_S \ll 1$, then s_1 will be a slow variable over the T_{s_2} timescale, and thus we will expect s_1 to be essentially constant over the time course of the indicator reaction. In addition, let us assume that $T_{s_2} \gg t_{c_1}$, in which case c_1 will be on the order of its maximum value on the T_{s_2} timescale. Combining these observations leads to the approximation

$$s_1 = s_1^0 + \mathcal{O}(\delta_S), \quad t \leq T_{s_2} \tag{39a}$$

$$c_1 = \varepsilon s_1^0 + \mathcal{O}(\delta_S), \quad t \leq T_{s_2} \tag{39b}$$

to the non-observable reaction over the timescale T_{s_2}. Equations (39a) and (39b) seem to suggest that $e_2^A \ll 1$ over the T_{s_2} timescale. Furthermore, since the changes in s_1 and c_1 are comparatively minimal when $t_{c_1} \leq t \leq T_{s_2}$, the production of e_2^A is effectively constant over the T_{s_2} timescale

$$\dot{e}_2^A \approx \varepsilon k_2 s_1^0 \equiv \varpi. \tag{40}$$

Integration of (40) yields the following approximation of e_2^A on the T_{s_2} timescale

$$e_2^A \approx \int_0^t \varpi \, \mathrm{d}u = \varpi t, \tag{41}$$

where u is a dummy variable. The approximate average value $\langle e_2^A \rangle$ on T_{s_2} is easily obtainable through straightforward integration

$$\langle e_2^A \rangle = \frac{\varpi}{T_{s_2}} \int_0^{T_{s_2}} t \, \mathrm{d}t = \frac{1}{2} T_{s_2} \varpi, \tag{42}$$

and inserting (42) into (30) yields the following estimate for T_{s_2}:

$$T_{s_2} = \sqrt{\frac{2(K_{M_2} + s_2^0)}{k_4 \varpi}} \equiv T_{s_2}^*. \tag{43}$$

We can write (43 in a slightly more convenient form. Defining the *limiting* slow timescale $t_{s_2}^*$ as

$$t_{s_2}^* \equiv \frac{K_{M_2} + s_2^0}{V_2}, \tag{44}$$

allows us to express $T_{s_2}^\star$ as

$$T_{s_2}^* = \sqrt{2 t_{s_1} t_{s_2}^*}. \tag{45}$$

We expect $T_{s_2}^*$ to provide an accurate estimate for total completion time of the indicator reaction as long as the non-observable reaction is comparatively slow. For a generic (and linear) dynamical system of the form

$$\dot{x} = -ax, \quad x(0) = x_0 \tag{46}$$

the depletion or *characteristic* timescale is $1/a$, and thus we look for a timescale that is indicative of the time it takes for the initial quantity (i.e., x_0 in the context of (46)) to deplete to an amount that is less than or equal to x_0/e. Following suit from the linear theory, we will consider the timescale $T_{s_2}^*$ to be a sufficient depletion timescale as long as

$$s_2(T_{s_2}^*) \leq s_2^0/e \approx 0.37 s_2^0. \tag{47}$$

Numerical solutions of the mass action equations confirm the validity of the timescale $T_{s_2}^*$ when the indicator reaction is much faster than the non-observable reaction provided $t_{c_1} \ll T_{s_2}^*$ (see FIGURES 2a and 2b).

Next, we want to develop an asymptotic solution to the mass action equations that will be valid when: (1) $T_{s_2}^*$ is an accurate and precise depletion timescale, (2) the concentrations s_1 and c_1 remain on the order of their maximum values (s_1^0 and εs_1^0 respectively) for the duration of the indicator reaction, and (3) the fast timescale t_{c_1} is negligibly short. To begin, let us assume that

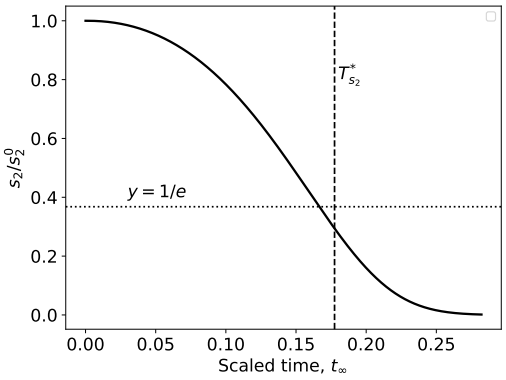

(a)

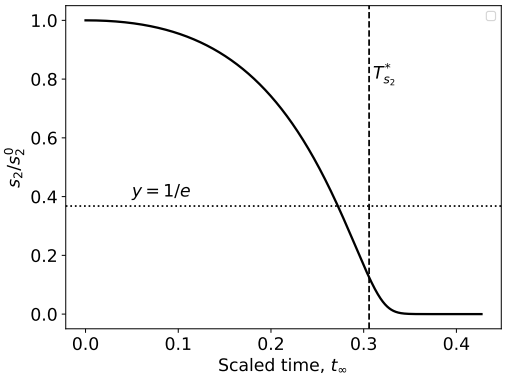

(b)

Figure 2: The accuracy of the timescale $T^*_{s_2}$ when the indicator reaction (2) is fast ($\delta_S \ll 1$). The solid black curves numerical solutions to the mass action equations of the complete reaction. The dashed line marks the timescale $T^*_{s_2}$ and the dotted line represents the quantity $1/e$. (a) The constants (without units) used in the numerical simulation are: $e_1^0 = 1, s_1^0 = 100, k_1 = 1, k_2 = 1$ and $k_{-1} = 1$. $s_2^0 = 10$, $k_3 = 10, k_4 = 100$ and $k_{-3} = 10$. (b) The constants (without units) used in the numerical simulation are: $e_1^0 = 1, s_1^0 = 100, k_1 = 1, k_2 = 1$ and $k_{-1} = 1$. $s_2^0 = 100$, $k_3 = 10, k_4 = 100$ and $k_{-3} = 10$. In both cases, we see that the timescale $T^*_{s_2}$ yields an accurate approximation to the completion time of the indicator reaction. Time has been mapped to the t_∞ scale: $t_\infty(t) = 1 - 1/\ln(t + e)$.

the initial concentration s_2^0 is large enough so that

$$\max_{t \leq T^*_{s_2}} e_2^A \ll s_2^0, \tag{48}$$

in which case we can assume $\lambda \ll 1$. Then, from Tikhonov's theorem, and due to the existence of the slow manifold $\mathcal{M}_\lambda$, we have

$$c_2 = \frac{e_2^A}{K_{M_2} + s_2} s_2 + \mathcal{O}(1) \tag{49}$$

as a leading order approximation. Insertion of this approximation into the mass action equation for s_2 yields

$$\dot{s}_2 = -\frac{k_4 e_2^A}{K_{M_2} + s_2} s_2 + \mathcal{O}(1). \tag{50}$$

Substitution of $e_2^A \approx \varpi t$ into (50) gives us

$$\dot{s}_2 = -\frac{k_4 \varpi t}{K_{M_2} + s_2} s_2 + \mathcal{O}(1) \tag{51}$$

as our final asymptotic approximation to the differential equations governing the temporal depletion of s_2. Equation (51) has a closed-form solution in the form of the Schnell–Mendoza equation

$$s_2 = K_{M_2} W \left[\sigma_2 \exp\left(\sigma_2 - \frac{k_4 \varpi t^2}{2 K_{M_2}} \right) \right], \tag{52}$$

and provides an accurate approximation to the mass action model (see FIGURES 3a and 3b).

4.2. Case 2: The indicator reaction is roughly the same speed as the non-observable reaction ($\delta \approx 1$)

It is instinctive, in the case that the non-observable reaction and the indicator reaction both complete at roughly the same time, to use either the slow timescale, t_{s_1} or T_{s_2}, as the depletion timescale for the complete reaction. Of course, given our earlier definition of the timescale T_{s_2}

$$T_{s_2} = \frac{K_{M_2} + s_2^0}{k_4 \langle e_2^A \rangle}, \tag{53}$$

we can formulate a nonlinear algebraic equation that will allow us to compute an estimate for the depletion timescale when the reactions are equivalent in

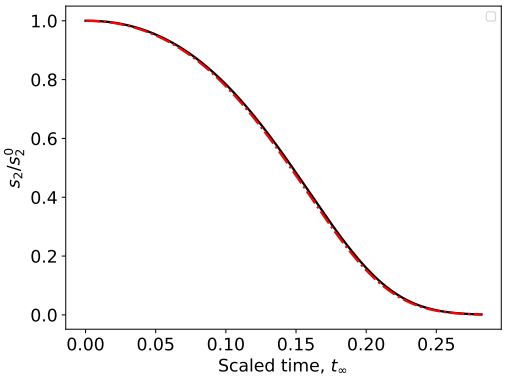

(a)

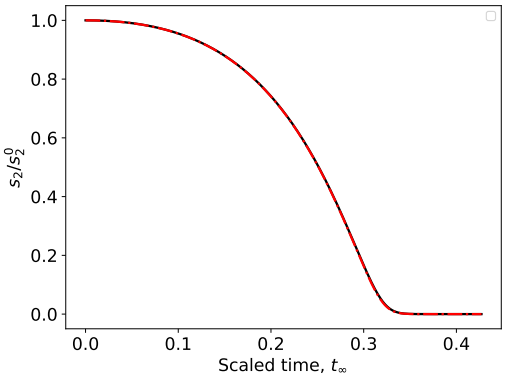

(b)

Figure 3: The leading order asymptotic solution (52) of the substrate concentration for the indicator reaction matches the numerical solution when the indicator reaction is faster than the non-observable reaction ($\delta_S \ll 1$). The solid black curves numerical solutions to the mass action equations of the complete reaction (8) and the broken red curves are numerical solutions to the asymptotic differential equation (51). (a) The constants (without units) used in the numerical simulation are: $e_1^0 = 1, s_1^0 = 100, k_1 = 1, k_2 = 1$ and $k_{-1} = 1$. $s_2^0 = 10$, $k_3 = 10, k_4 = 100$ and $k_{-3} = 10$. (b) The constants (without units) used in the numerical simulation are: $e_1^0 = 1, s_1^0 = 100, k_1 = 1, k_2 = 1$ and $k_{-1} = 1$. $s_2^0 = 100$, $k_3 = 10, k_4 = 100$ and $k_{-3} = 10$. Time has been mapped to the t_∞ scale: $t_\infty(t) = 1 - 1/\ln(t + e)$.

speed. First,

$$\langle e_2^A \rangle = \frac{1}{T_{s_2}} \int_0^{T_{s_2}} (s_1^0 - s_1 - c_1)\, \mathrm{d}t, \tag{54}$$

and thus we see that T_{s_2} should satisfy

$$\int_0^{T_{s_2}} (s_1^0 - s_1 - c_1)\,\mathrm{d}t = \frac{K_{M_2} + s_2^0}{k_4}. \tag{55}$$

Second, under the RSA, the concentration c_1 is expressible (algebraically) in terms of s_1, and therefore

$$\int_0^{T_{s_2}} (s_1^0 - s_1 - c_1)\,\mathrm{d}t \approx \int_0^{T_{s_2}} \frac{(K_{M_1} + s_1)\Delta s_1 - e_1^0 s_1}{K_{M_1} + s_1}\,\mathrm{d}t, \tag{56}$$

where $\Delta s_1 = s_1^0 - s_1$ (the timescale t_{c_1} has been assumed to be negligibly small and hence left out of the integrand, although it is straightforward to include this term). Third, the definite integral on the right hand side of (56) is straightforward to compute analytically; evaluating it will yield a nonlinear equation in terms of the variable T_{s_2}, and the solution to (55) can be approximated by using a standard contraction mapping algorithm. Using the average $\langle e_2^A \rangle$ provides an accurate estimate of the slow (depletion) timescale (see FIGURE 4).

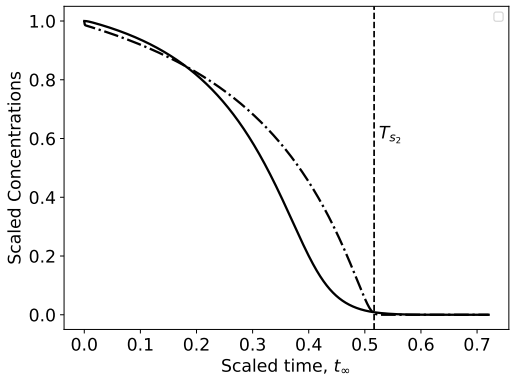

Figure 4: The averaging method for the estimation of the depletion timescale for the indicator substrate is still valid when the non-observable and indicator reactions occur at roughly the same speed ($\delta_S \approx 1$). The solid black curve is the numerically-computed depletion curve of s_2 and the dotted/dashed black curve is the numerically-integrated depletion curve of s_1. In this numerical simulation $k_3 = 1, k_4 = 1, k_{-3} = 10, s_2^0 = 70$, and $k_1 = 10, k_2 = 15, k_{-1} = 1, e_1^0 = 1$ and $s_1^0 = 70$. Both substrates have been scaled as s_2/s_2^0 and s_1/s_1^0. Time has been mapped to the t_∞ scale: $t_\infty(t) = 1 - 1/\ln(t + e)$.

From a practical point of view, the utility in estimating T_{s_2} through a contraction mapping is rather minimal. The objective here will be to construct a criteria from which a reduced model can be be extracted from the mass action equations that will be valid without any *a priori* knowledge of the intrinsic timescales of the indicator reaction (or the non-observable reaction). To do this, let us first revisit the generic scaling introduced in the previous section:

$$\frac{d\bar{s}_2}{dT} = \frac{\max e_2^A}{\langle e_2^A \rangle} \frac{(1+\kappa_2)(1+\sigma_2)}{\delta_S} \left[\left(\frac{\sigma_2}{1+\sigma_2} \bar{c}_2 - \bar{e}_2^A \right) \bar{s}_2 + \frac{\alpha}{1+\sigma_2} \bar{c}_2 \right] \tag{57a}$$

$$\lambda \frac{d\bar{c}_2}{dT} = \frac{\max e_2^A}{\langle e_2^A \rangle} \frac{(1+\kappa_2)(1+\sigma_2)}{\delta_S} \left[\left(\bar{e}_2^A - \frac{\sigma_2}{1+\sigma_2} \bar{c}_2 \right) \bar{s}_2 - \frac{1}{1+\sigma_2} \bar{c}_2 \right]. \tag{57b}$$

Bearing in mind that it is assumed that $\delta_S \approx 1$, it is sufficient (but not necessary) to bound λ in order to assemble a dynamical model that can be reduced (asymptotically) through slow manifold projection. The upper bound on λ, which we denote as $\lambda^{\max}$, is

$$\lambda \leq \lambda^{\max} \equiv \frac{s_1^0}{K_{M_2} + s_2^0}. \tag{58}$$

The parameter $\lambda^{\max}$ is the natural small parameter when the indicator is very slow. Furthermore, if the non-observable reaction completes very quickly relative to the non-observable reaction, and $\delta_S \ll 1$, then the average available enzyme should be on the order of s_1^0:

$$\langle e_2^A \rangle = \frac{1}{T_{s_2}} \int_0^{T_{s_2}} e_2^A \, \mathrm{d}t \sim s_1^0. \tag{59}$$

Thus, if $s_2^0 \gg s_1^0$, then the approximation

$$\dot{s}_2 = -\frac{k_4 e_2^A}{K_{M_2} + s_2} s_2 + \mathcal{O}(1) \tag{60}$$

will be valid regardless of the relative speeds of the reactions when $\lambda^{\max} \ll 1$. Furthermore, (60) admits a closed-form solution using separation of variables that consists of composite Lambert-W functions (we do not present this expression here, although we remark that it is straightforward, albeit somewhat

tedious to derive). Under the RSA, we obtain

$$\dot{s}_2 = -\left(\frac{(K_{M_1} + s_1)\Delta s_1 - e_1^0 s_1}{K_{M_1} + s_1}\right)\left(\frac{k_4}{K_{M_2} + s_2}\right)s_2 \tag{61}$$

as the final form of our reduced differential equation for $\dot{s}_2$.

4.3. Case 3: The indicator reaction is much slower than the non-observable reaction ($\delta_S \gg 1$)

We now consider the case when $\delta_S \gg 1$, and the completion of the non-observable occurs much sooner than the completion of the indicator reaction. As mentioned in the previous subsection, a very slow indicator reaction suggests that s_2 will be slow over the timescale t_{s_1}. Consequently, we can approximate s_2 as

$$s_2 = s_2^0, \quad t < t_{s_1}. \tag{62}$$

Furthermore, because the non-observable reaction has effectively completed when $t = t_{s_1}$, we can approximate $\Delta s_1 = s_1^0$ when $t \geq t_{s_1}$, in which case

$$\dot{s}_2 = -\frac{k_4 s_1^0}{K_{M_2} + s_2}s_2 + \mathcal{O}(1), \quad t \geq t_{s_1}. \tag{63}$$

Equation (63) can be integrated directly to yield a Schnell–Mendoza equation for s_2:

$$s_2 = K_{M_2} W\left[\sigma_2 \exp(\sigma_2 - \eta_2(t))\right], \quad t \geq t_{s_1}. \tag{64}$$

The validity of the approximate solution (62) can be established by the mathematical formulation of the RSA for the indicator reaction. If $s_2 \approx s_2^0$ over the interval $[0, t_{s_1}]$, then

$$\max_{t \leq t_{s_1}} |\dot{s}_2| \cdot t_{s_1} \ll s_2^0. \tag{65}$$

The inequality given in (65) translates to

$$\delta_S \gg (\sigma_2 + 1)(\kappa_2 + 1), \tag{66}$$

with $\max \dot{s}_2 = k_3 s_1^0 s_2^0$. In the case of a slow indicator reaction, we expect that $T_{s_2} = t_{s_2}^*$. Thus, we have a RSA that is pertinent to the indicator reaction

$$\frac{V_1}{V_2} \gg \frac{K_{M_1}}{K_{M_2}}(1 + \sigma_1)(1 + \kappa_2), \tag{67}$$

and establishes a region of validity for the solution to the mass action equations during the initial build-up of c_2 when $t \leq t_{s_1}$. Equation (67) is analogous to the term used to measure the strength of fully competitive enzyme reactions with alternative substrates [26, 27]. Numerical simulations (see FIGURE 5) confirm the validity of $t^*_{s_2}$ and (63).

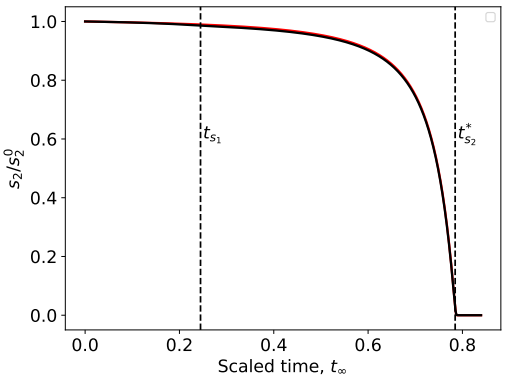

Figure 5: Validity of the timescale $t^*_{s_2}$ and the reduced ordinary differential equation given by (63) for the substrate depletion of the indicator reaction when the indicator reaction is much slower than the non-observable reaction ($\delta_S \gg 1$). The solid black curve in the numerical solution to the mass action equations (8) and the solid red curve corresponds to the numerical solution to (63) extended to $t \geq 0$. In this numerical simulation $k_3 = 0.1, k_4 = 1, k_{-3} = 10, s_2^0 = 10000$, and $k_1 = 25, k_2 = 100, k_{-1} = 1, e_1^0 = 1$ and $s_1^0 = 100$. The respective values of $\lambda^{\max}$ and δ_S are ≈ 0.009 and ≈ 0.01. Time has been mapped to the t_∞ scale: $t_\infty(t) = 1 - 1/\ln(t + e)$.

5. Estimate of lag time of the indicator reaction

Up until this point, we have not mentioned the equivalent of a fast timescale that is pertinent to the indicator reaction. In the case of the non-observable reaction, the fast timescale corresponds to the time it takes the reaction to reach QSS. However, based on our scaling analysis, we have demonstrated that a QSSA can be imposed for the complete duration of the reaction as long as $\lambda \ll 1$. At first glance, it would seem that the kinetics of the indicator reaction omit the influence of a fast timescale. This is however false. To derive the fast

timescale, we will assume that initial conditions are *not* experimental, and that the indicator reaction is equipped with a non-trivial amount of complex c_2^0 at the start of the reaction. Furthermore, we will assume that the substrate, s_2 does not deplete significantly over the duration of the fast timescale. Denoting the fast timescale as t_{c_2}, the mass action equation can be linearized:

$$\dot{c}_2 = k_3(e_2^A - c_2)s_2^0 - (k_{-3} + k_4)s_2^0, \quad t \leq t_{c_2} \tag{68a}$$

$$c_2(0) = c_2^0. \tag{68b}$$

The solution to the linear equation (68) is given by Duhamel's Principle

$$c_2(t) = \exp(-\mu t)c_2^0 + \int_0^t \exp(\mu(s-t))\ e_2^A(s)\ ds, \quad \mu \equiv k_3(K_{M_2} + s_2^0), \tag{69}$$

and thus, the naturally occurring characteristic timescale is $1/\mu$:

$$t_{c_2} \equiv \frac{1}{k_3(K_{M_2} + s_2^0)}. \tag{70}$$

If initial conditions are not experimental, then t_{c_2} provides a reasonable estimate on the time it takes for the indicator reaction to reach QSS. However, since typical experimental initial conditions start on the c_2-nullcline, we turn to scaling to provide a biochemical interpretation of the timescale t_{c_2}. Defining $T^* = t/t_{c_2}$, we obtain:

$$\frac{d\bar{s}_2}{dT^*} = \lambda \left[\left(\frac{\sigma_2}{1+\sigma_2}\bar{c}_2 - \bar{e}_2^A \right)\bar{s}_2 + \frac{\alpha}{1+\sigma_2}\bar{c}_2 \right] \tag{71a}$$

$$\frac{d\bar{c}_2}{dT^*} = \left(\bar{e}_2^A - \frac{\sigma_2}{1+\sigma_2}\bar{c}_2 \right)\bar{s}_2 - \frac{1}{1+\sigma_2}\bar{c}_2. \tag{71b}$$

We see from the scaling that t_{c_2} defines a *lag* timescale when experimental initial conditions are prescribed. Over this timescale, the indicator reaction is effectively stationary, since both c_2 and s_2 are slow variables (c_2 is a slow variable not from scaling, but because it will stay near the c_2-nullcline over short timescales, and thus $\dot{c}_2 \approx 0$ when $t \leq t_{c_2}$). Thus, the fast timescale of the indicator reaction defines the lag time of the reaction. The lag time is present

due to the fact that the indicator reaction cannot "start" until after a non-trivial amount of enzyme E_2 has been produced in the non-observable reaction.

The relationship between λ, t_{c_2} and T_{s_2} is now evident. The ratio of fast and slow timescales is bounded above by λ,

$$\frac{t_{c_2}}{T_{s_2}} < \lambda. \tag{72}$$

The strict inequality follows from the fact that,

$$\frac{t_{c_2}}{T_{s_2}} = \frac{\bar{\lambda}}{(1+\sigma_2)(1+\kappa_2)} \tag{73}$$

where $\bar{\lambda}$ is given by

$$\bar{\lambda} \equiv \frac{\langle e_2^A \rangle}{K_{M_2} + s_2^0}. \tag{74}$$

Furthermore, since $\langle e_2^A \rangle \leq \max e_2^A$, we have that

$$\bar{\lambda} \leq \lambda \tag{75}$$

from which (72) follows.

To explore the relationship between the QSSA and the RSA, we note that the parameter $\lambda^{\max}$ is easily derived using Segel's heuristic approach [22]:

$$\max |\dot{s}_2| \cdot t_{c_2} \ll s_2^0 \rightarrow \lambda^{\max} \ll 1 \tag{76}$$

Since it is clear that

$$\bar{\lambda} \leq \lambda \leq \lambda^{\max}, \tag{77}$$

it follows that the RSA (i.e., $\lambda^{\max} \ll 1$) ensures separation of fast and slow timescales; consequently, the RSA for the indicator reaction implies the QSSA and is thus a universal qualifier for the validity of the reduced model.

6. Discussion

The primary contribution of this paper is to introduce methods for the appropriate scaling and timescale estimates of the auxiliary enzyme assay. The

identification of specific parameters through scaling has yielded necessary and sufficient conditions for the QSSA, whereas previous nonlinear studies of the coagulation cascade with auxiliary enzymes have employed the QSSA without justification [10]. Moreover, previous analyses [8] dot not provide insight as to how to properly estimate kinetic timescales via nonlinear methods, even though the coupled enzyme auxiliary assays are inherently nonlinear. This work outlines a clear procedure for estimating depletion timescales, and serves as a template for the analysis of more complicated reactions. We give a brief summary of the results of the analysis in what follows.

Scaling analysis of the mass action equations that model the kinetics of a coupled auxiliary enzyme reaction (1)–(2) has revealed two small parameters, ε and $\lambda^{\max}$,

$$\lambda^{\max} = \frac{s_1^0}{K_{M_2} + s_2^0} \ll 1$$
$$\varepsilon = \frac{e_1^0}{K_{M_1} + s_1^0} \ll 1.$$

The parameters ε and λ regulate the partition of the slow timescales t_{c_1}, t_{c_2} and the fast timescales t_{s_1} and T_{s_2}:

$$\frac{t_{c_1}}{t_{s_1}} < \varepsilon, \quad \frac{t_{c_2}}{T_{s_2}} < \lambda \leq \lambda^{\max}. \tag{79}$$

When these parameters are small, and the timescales t_{c_2} and t_{s_1} are adequately separated, the indicator reaction can be assumed to be in a QSS for the duration of the reaction (i.e, for $t \geq 0$). There is a twofold reasoning to this assumption. First, if $\lambda^{\max} \ll 1$, then

$$\lambda \equiv \frac{\max e_2^A}{K_{M_2} + s_2^0} \ll 1,$$

and model reduction from slow manifold projection is valid regardless of which reaction finishes first (non-observable or indicator). Since it is not generally possible to determine which reaction is faster in the typical experiment *a priori*, the condition that $\lambda^{\max} \ll 1$ serves as a *sufficient* qualifier to ensure the validity

of the reduced model for the reaction rate of depletion of the indicator substrate:

$$\dot{s}_2 = -\left(\frac{(K_{M_1} + s_1)\Delta s_1 - e_1^0 s_1}{K_{M_1} + s_1}\right)\left(\frac{k_4}{K_{M_2} + s_2}\right)s_2.$$

Second, as long as $t_{c_2} \ll t_{s_1}$, a QSSA will *effectively* hold for all time since experimental initial conditions lie on the c_2-nullcline. From the theory of singular perturbations, the slow manifold, "$\mathcal{M}_\lambda$," is an invariant manifold that is well-approximated by the c_2-nullcline when $\lambda^{\max} \ll 1$. Because experimental initial conditions lie on the c_2-nullcline, the phase-space trajectory is already extremely close to the slow manifold, and therefore there is no need for an initial fast transient in order for the trajectory to reach the slow manifold. As we have pointed out, the slow manifolds is a geometrical representation of the steady-state rate equation for the reaction. Note that this is very different from the non-observable reaction, since a fast transient (the duration of the fast transient is approximated by the timescale t_{c_1}) must elapse before the QSSA is justifiable.

In addition, simple asymptotic solutions to the mass action equations were derived that are valid when the indicator reaction is very fast or very slow in comparison to the non-observable reaction. If the indicator reaction is fast, then the time course of the indicator substrate s_2 is accurately model by

$$s_2 = K_{M_2} W\left[\sigma_2 \exp\left(\sigma_2 - \frac{k_4 \varpi t^2}{2K_{M_2}}\right)\right],$$

where W denotes the Lambert-W function. In contrast, if the indicator reaction is very slow, then the time course of s_2 can be modeled by

$$s_2 = K_{M_2} W\left[\sigma_2 \exp\left(\sigma_2 - \frac{V_2 t}{K_{M_2}}\right)\right].$$

Note that the above two expressions are analogous to the Schnell–Mendoza equation [18].

It should be pointed out that the condition $\lambda^{\max} \ll 1$, which can be ensured by requiring an excess of the initial amount of substrate s_2 (i.e., requiring that s_2^0 be large enough so that $s_1^0 \ll s_2^0$), is sufficient but not necessary for the

validity of the reduced model presented in (61). In general, it is desirable that s_2^0 be much larger than the maximum of amount of e_2^A over the timescale of the indicator reaction. If the indicator reaction is fast, then the maximum amount of available enzyme, $\max e_2^A$, will be small, and thus the requirement that $s_1^0 \ll s_2^0$ is unnecessary as if $\max e_2^A \ll K_{M_2}$ (see FIGURE 6). Of course, the integrity of the reduced model does not diminish if $s_1^0 \ll s_2^0$; therefore, the qualifier, $\lambda^{\max} \ll 1$, is a universal condition for the validity of (61), as this will ensure that $\max e_2^A \ll s_2^0$ on any timescale.

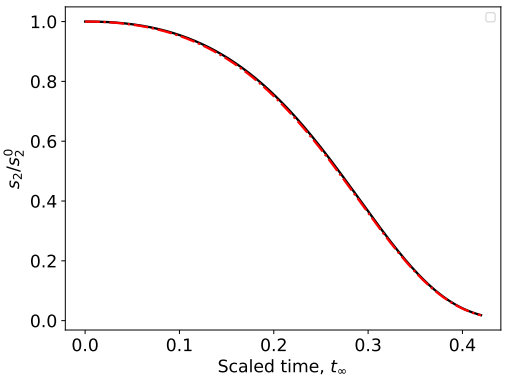

Figure 6: The condition that $\lambda \ll 1$ is necessary for slow manifold projection, while the condition $\lambda^{\max} \ll 1$ is merely sufficient. The solid black curve is the numerical solution to the mass action equations and the broken red curve is to the numerical solution to (61). In this simulation $k_3 = 1, k_4 = 100, k_{-3} = 10, s_2^0 = 1$, and $k_1 = 1, k_2 = 1, k_{-1} = 1, e_1^0 = 1$ and $s_1^0 = 100$. $s_1^0/s_2^0 \approx 100$ and $\lambda^{\max} \approx 1$. However, $\max e_2^A \approx 1.543$ and therefore $\lambda \approx 0.014 \ll 1$. Time has been mapped to the t_∞ scale: $t_\infty(t) = 1 - 1/\ln(t + e)$.

Finally, three reduced models have been derived that can be utilized in the inverse problem. Our analysis seems suggests that a fast indicator reaction is the most beneficial case for parameter estimation. Under this circumstance, two expressions

$$s_2 = K_{M_2} W\left[\sigma_2 \exp\left(\sigma_2 - \frac{V_2 V_1 t^2}{2K_{M_2}(s_1^0 + K_{M_1})}\right)\right],$$

and

$$s_2 = -\int_{t_{c_1}}^{t} \left(\frac{(K_{M_1} + s_1)\Delta s_1 - e_1^0 s_1}{K_{M_1} + s_1} \right) \left(\frac{k_4}{K_{M_2} + s_2} s_2 \right) \mathrm{d}u$$

can be simultaneously utilized to estimate the four unknown parameters V_1, V_2, K_{M_1}, and K_{M_2}. The full analysis of the inverse problem is beyond the scope of this paper; we hope, however, to theoretically investigate the scope of parameter estimation in coupled auxiliary enzyme assays in subsequent future work.

Acknowledgements

We are grateful to Dr. Enrico DiCera (Saint Louis University School of Medicine) for his suggestions to explore this problem. We are also grateful to Dr. Antonio Baici (University of Zurich) for helpful discussions about this work during the 2017 Beilstein Enzymology Symposia (Rüdesheim, Germany). This work is partially supported by the University of Michigan Protein Folding Diseases Initiative, and Beilstein-Institut zur Förderung der Chemischen Wissenschaften through its Beilstein Enzymology Symposia. Dr. Stroberg is a fellow of the Michigan IRACDA program (NIH/NIGMS grant: K12 GM111725).

References

[1] F. B. Rudolph, B. W. Baugher, R. S. Beissner, Techniques in coupled enzyme assays, Methods Enzymol. 63 (1979) 22–42.

[2] B. A. C. Storer, A. Cornish-bowden, P. O. Box, B. Birmingham, The kinetics of coupled enzyme reactions, Biochem. J. 141 (1974) 205–209.

[3] W. W. Cleland, Optimizing coupled enzyme assays, Anal. Biochem. 99 (1979) 142–145.

[4] W. R. McClure, Kinetic analysis of coupled enzyme assays, Biochemistry 8 (1969) 2782–2786.

[5] J. S. Easterby, Coupled enzyme assays: A general expression for the transient, Biochim Biophys Acta. 293 (1973) 552–558.

[6] L. Michaelis, M. L. Menten, Die Kinetik der Invertinwirkung, Biochem. Z. 49 (1913) 333–369.

[7] O. D Dang, A. Vindigni, E. Di Cera, An allosteric switch controls the procoagulant and anticoagulant activities of thrombin, Proc. Natl. Acad. Sci. USA 92 (1995) 5977–81.

[8] F. Martorana, A. Moro, On the kinetics of enzyme amplifier systems with negative feedback, Math. Biosci. 21 (1974) 77–84.

[9] E. Beltrami, J. Jesty, Mathematical analysis of activation thresholds in enzyme-catalyzed positive feedbacks: application to the feedbacks of blood coagulation, Proc. Natl. Acad. Sci. USA 92 (1995) 8744–8748.

[10] M. Khanin, V. Semenov, A mathematical model of the kinetics of blood coagulation, J. theor. Biol. 136 (1989) 127–134.

[11] W. Stroberg, S. Schnell, On the estimation errors of K_M and V from time-course experiments using the Michaelis-Menten equation, Biophys. Chem. 219 (2016) 17–27.

[12] W. Stroberg, S. Schnell, On the validity and errors of the pseudo-first-order kinetics in ligandreceptor binding, Math. Biosci. 287 (2017) 3–11.

[13] W. Klonowski, Simplifying principles for chemical and enzyme kinetics, Biophys. Chem. 18 (1983) 73–87.

[14] J. F. Griffiths, Reduced kinetic models and their application to practical combustion systems, Prog. Energy Combust. Sci. 21 (1995) 25–107.

[15] M. S. Okino, M. L. Mavrovouniotis, Simplification of mathematical models in chemical reaction systems, Chem. Rev. 98 (1998) 391–408.

[16] R. Bertram, J. E. Rubin, Multi-timescale systems and fast-slow analysis, Math. Biosci. 287 (2017) 105–121.

[17] S. Schnell, C. Mendoza, The condition for pseudo-first-order kinetics in enzymatic reactions is independent of the initial enzyme concentration, Biophys. Chem. 107 (2004) 165–174.

[18] S. Schnell, C. Mendoza, Closed form solution for time-dependent enzyme kinetics, J. Theor. Biol. 187 (1997) 207–212.

[19] A. H. Nguyen, S. J. Fraser, Geometrical picture of reaction in enzyme kinetics, J. Chem. Phys. 91 (1989) 186–193.

[20] M. R. Roussel, S. J. Fraser, Geometry of the steady-state approximation: Perturbation and accelerated convergence methods, J. Chem. Phys. 93 (1990) 1072–1081.

[21] S. M. Hanson, S. Schnell, Reactant stationary approximation in enzyme kinetics, J. Phys. Chem. A 112 (2008) 8654–8658.

[22] L. A. Segel, On the validity of the steady state assumption of enzyme kinetics, Bull. Math. Biol. 50 (1988) 579–593.

[23] S. K. Shoffner, S. Schnell, Approaches for the estimation of timescales in nonlinear dynamical systems: Timescale separation in enzyme kinetics as a case study, Math. Biosci. 287 (2017) 122–129.

[24] L. A. Segel, M. Slemrod, The quasi-steady-state assumption: a case study in perturbation, SIAM Rev. 31 (1989) 446–477.

[25] S. Schnell, Validity of the Michaelis-Menten equation – Steady-state, or reactant stationary assumption: that is the question, FEBS J. 281 (2014) 464–472.

[26] S. Schnell, C. Mendoza, Time-dependent closed form solutions for fully competitive enzyme reactions, Bull. Math. Biol. 62 (2000) 321–336.

[27] S. Schnell, C. Mendoza, Enzyme kinetics of multiple alternative substrates, J. Math. Chem. 27 (2000) 155–170.